

Evidence of ferromagnetic quantum phase transition in  $\text{Ba}_{1-x}\text{Sr}_x\text{VS}_3$ Andrea Gauzzi<sup>1</sup>, Neven Barisić<sup>2</sup>, Francesca Lioci<sup>1</sup>, Gianluca Calestani<sup>3</sup>,Fulvio Bolzoni<sup>1</sup>, Patrik Fazekas<sup>4</sup>, Edi Gilioli<sup>1</sup>, and László Forró<sup>2</sup><sup>1</sup>IMEM-CNR, Area delle Scienze, 43010 Parma, Italy<sup>2</sup>Institut de Physique de la Matière Complexe, EPFL, CH-1015 Lausanne, Switzerland<sup>3</sup>Dipartimento di Chimica, Università di Parma, Area delle Scienze, 43100 Parma, Italy<sup>4</sup>Research Institute for Solid State Physics and Optics, P.O. Box 49, H-1525 Budapest, Hungary

(dated: February 8, 2022)

Resistivity under pressure and magnetization measurements on  $\text{Ba}_{1-x}\text{Sr}_x\text{VS}_3$  single crystals with  $0 < x < 0.18$  and no sulphur deficiency show an abrupt onset of ferromagnetic (FM) order at a critical value  $x = 0.07$ , concomitant to a change of the magnetic properties at the metal-insulator transition (MIT) and to a collapse of the unit cell at ambient temperature. A reduction of the MIT temperature to 50 K upon  $x$  that scales as the V-S distance is also observed. This gives evidence of a chemical pressure induced quantum phase transition that stabilizes the incipient FM order of  $\text{BaVS}_3$ . The  $0.07 < x$  results suggest a coexistence of FM and metallic phases at larger  $x$ .

PACS numbers: 71.30.+h, 71.27.+a, 75.50.-y

Keywords:

The hexagonal perovskite  $\text{BaVS}_3$  [1] displays a manifold of magnetic, transport and structural properties driven by  $3d(V^{4+})$  electron correlations. In the high temperature metallic phase, it consists of hexagonal closed packed chains of face-sharing  $\text{VS}_6$  octahedra. The MI transition  $T_{MI} = 69$  K is preceded by a zigzag of the chains at 240 K leading to an orthorhombic structure [3].  $T_{MI}$  decreases under pressure and the insulating phase is suppressed for  $P > 2$  GPa [2]. In stoichiometric compounds ( $\delta = 0$ ), the ambient pressure transition is concomitant to an AF-like cusp of the magnetic susceptibility, [1], and to a 2 $\times$ 2 superstructure along the chains [4, 5]. A neutron scattering study [6] reported a long range AF-like order in the ab-plane and an intrachain ferromagnetic (FM) one at  $T_x = 30$  K, related to the cusp. Assuming a large number of degenerate configurations of singlet pairs with different orbital symmetry in the triangular plane, a picture of spin-orbital liquid was proposed [6, 7]. A latent FM instability is apparent from the positive Weiss constant in the metallic phase and the FM behavior of sulphur-deficient samples [8]. In agreement with these experiments, ab initio calculations [9, 10] predict a dominant FM coupling along  $c$  and a comparatively weak AF one in the ab-plane, thus suggesting a ground state of FM chains with a nearly frustrated AF interchain coupling.

The origin of the MI transition and its relation with the magnetic and orbital orderings remain controversial. Overlapping wide and narrow  $d$ -bands were recently observed by ARPES [11]. A simple tight-binding model explaining the physical properties at the MI transition includes a broad  $A_{1g}$  band arising

from the direct overlap of  $3d_{z^2}$  orbitals along the  $c$ -axis, and a doubly degenerate  $E_g$  narrow band created by the small V ( $3d$ )-S ( $3p$ ) hybridization [8, 15]. The width and relative occupancy of the bands remain to be determined experimentally. An X-ray diffraction study [5] suggests a nearly equal filling of the  $A_{1g}$  and  $E_g$  bands. A tuning mechanism for the occupancy of these two bands was recently proposed [12].

In this letter, we study the effects of chemical pressure on the magnetic, transport and structural properties of the system. At a critical value,  $x = 0.07$ , an abrupt onset of FM order is found concomitant to a disappearance of the AF-like cusp at the MI transition and to a collapse of the unit cell at room temperature. A progressive reduction of  $T_{MI}$  and smearing of the AF-like cusp with increasing  $x$  is also observed. The observation of a quantum phase transition (QPT) from a non-FM to a FM low-temperature state shows that the incipient FM order in the parent compound is stabilized by chemical pressure. The second result suggests a coexistence of FM and metallic phases at high pressure [15]. We discuss the possibility that the two phases coincide in the absence of disorder. We argue that the collapse of the unit cell is due to a sudden redistribution of electron charge between the relevant  $A_{1g}$  and  $E_{g1}$  bands.

A series of  $\text{Ba}_{1-x}\text{Sr}_x\text{VS}_3$  single crystals with  $x = 0.032, 0.053, 0.064, 0.068, 0.097, 0.126$ , and  $0.183$  were grown as described elsewhere using a solid state method [13]. Attempts to grow crystals with larger  $x$  values were unsuccessful. At  $x = 0.183$ , diffraction data indicate a significant amount of disorder and stacking faults, thus  $x = 0.18$  appears to be close to

the solubility limit. The needle-shaped crystals, 0.1 – 0.3 mm long, are aligned along the  $c$ -axis. The room temperature crystal structure, the Sr/Ba composition and the sulfur content were determined using X-ray diffraction. Within the experimental resolution, the crystal symmetry remains  $P6_3/mmc$  for all  $x$  values, as in the unsubstituted compound. The structural refinement indicates no sulfur deficiency for any  $x$  with a statistical uncertainty 0.05 or better. As a further check of the sulfur stoichiometry, a post-sulfurisation treatment in evacuated quartz ampoules at 450 °C for 3 days is found to affect neither the structural nor the physical properties. Thus, the results reported are exclusively ascribed to the Sr-induced chemical pressure.

The crystals were investigated by means of dc electrical resistivity under pressure,  $\rho_c(T;P)$ , up to 2 GPa, and dc magnetization,  $M(T)$ .  $\rho_c$  was measured in a four contact bar configuration in self-clamping pressure cells filled with kerosene as pressurizing agent. Since the needle-shaped crystals grow along the  $c$ -axis, the  $c$ -axis resistivity,  $\rho_c$ , was measured.  $M$  was measured in the zero-field and field-cooling (ZFC, FC) modes at 100 Oersted using a commercial RF SQUID magnetometer. Because of the small crystal size, the sample weight could not be determined. Yet, the sample sizes are comparable and the relative magnitude of  $M$  is significant.

A set of  $\rho_c(T;P)$  curves is shown in Fig. 1 for  $x=0.126$ . Similarly to the case of the unsubstituted compound [2] ( $x=0$ ), a progressive reduction of  $T_{MI}$  with increasing pressure is found.  $T_{MI}$  was estimated as the peak of the  $d\ln\rho_c/dT$  vs.  $T$  plot [2]. The effect of  $T_{MI}$  reduction with increasing  $x$  and with increasing pressure is apparent in the  $P$ – $T$  diagram of Fig. 2 that summarizes the  $\rho_c$  data. For  $x=0.12$ , the insulating state is suppressed at 1 GPa, i.e. half of the value for the unsubstituted compound [2]. By comparing the  $\rho_c(T;P)$  curves in the inset of Fig. 1, one notes that the  $T_{MI}$  reduction is accompanied by an increase of the slope,  $d\rho_c/dT$ , with increasing pressure. This trend is common to all samples and indicates a pressure-induced enhancement of the metallic properties, although the system remains a bad metal. By comparing the  $\rho_c(T)$  curves for different  $x$ , we observed that the residual resistivity increases with increasing  $x$  [14]. This trend indicates that the Sr-substitution creates a substantial amount of disorder, in agreement with diffraction data.

The  $T_{MI}$  reduction is correlated with the Sr-induced structural changes of the  $a$ - and  $c$ -axis as shown in Fig. 3. One notes that the smaller Sr ion induces a shrinking of the unit cell, as expected. Two

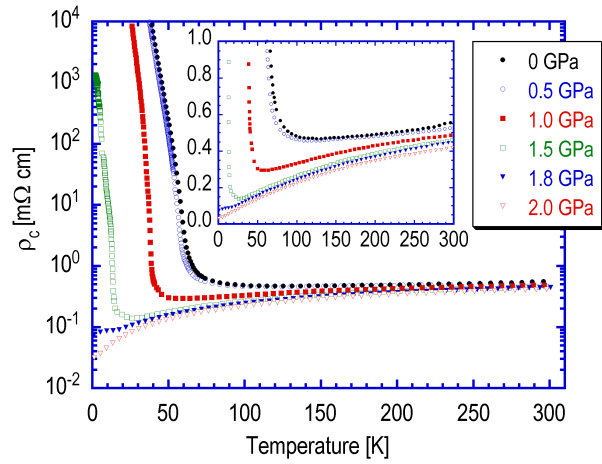


FIG. 1:  $c$ -axis resistivity curves as a function of temperature and pressure for  $x=0.126$ . One notes the steady reduction of the metal-insulator transition temperature  $T_{MI}$ , as pressure increases.

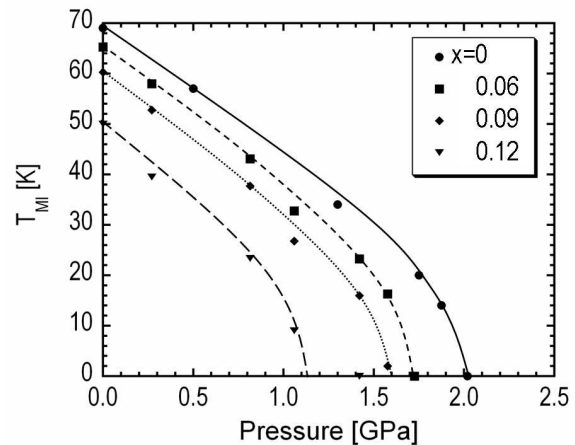


FIG. 2: Progressive reduction of  $T_{MI}$  upon  $x$  from the full set of the  $\rho_c(T;P)$  data. The  $x=0$  data are taken from ref. [2]. Lines are a guide to the eye.

features are though unusual: 1) at low substitution levels,  $x \leq 0.05$ , the shrinking is negligible; 2) at higher  $x$  values, the shrinking is large and occurs suddenly, first along the  $c$ -axis at  $x=0.07$  and then in the  $ab$ -plane at  $x=0.10$ . The latter shrinking is largest and corresponds to a collapse of the chains of  $VS_6$  octahedra one against the other. The  $c$ -axis increase at  $x \approx 0.10$  is consistent with the previous observation of disorder and stacking faults in this  $x$  range. In spite of this, the cell volume continues to decrease with  $x$ , for the shrinking of the  $a$ -axis dominates. The sudden drop of the  $a$ - and  $c$ -axis at  $x=0.07$  appears to be a

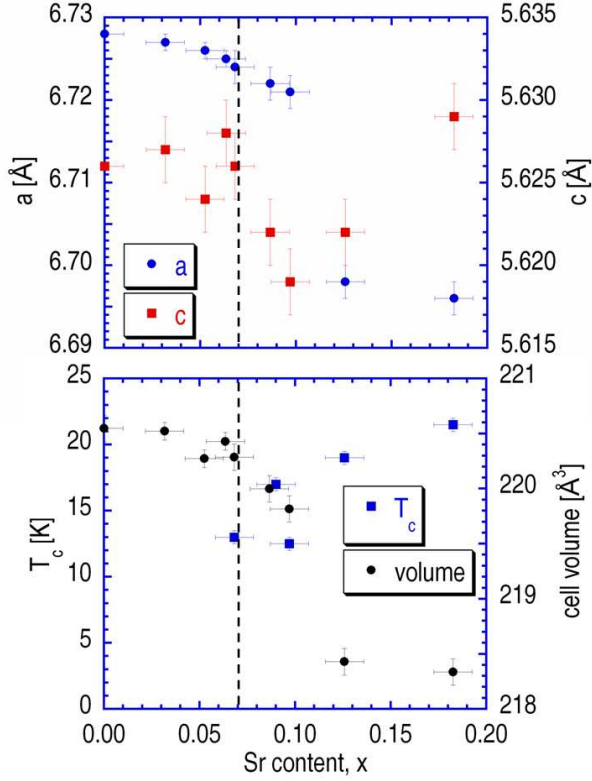


FIG. 3: Top panel:  $a$ - and  $c$ -axis variations of the hexagonal unit cell of  $\text{Ba}_{1-x}\text{Sr}_x\text{VS}_3$  with  $x$ . Note the drop of the  $c$ -axis at  $x = 0.07$  and the progressive reduction of the  $a$ -axis followed by a large drop at  $x = 0.10$ . Error bars are standard deviations of the data re-ment. Bottom panel: correlation between cell volume reduction and Curie temperature,  $T_c$ , and  $x$ . The vertical line at  $x = 0.07$  marks the onset of the cell volume drop and of the FM order.

room temperature signature of a phase transition at low temperature, as discussed below.

By analyzing the structural data, the V-S bond distance in the  $\text{VS}_6$  octahedra is found to be the only parameter that scales with  $T_{\text{MI}}$ . A linear regression of the  $T_{\text{MI}}$  vs. V-S data enables to predict that the M-I transition would be suppressed for V-S = 2.372 Å. This result is in agreement with the observation of  $T_{\text{MI}}$  reduction upon hydrostatic pressure [2]. One concludes that the volume reduction induced by either chemical or hydrostatic pressure stabilizes the metallic state. The  $T_{\text{MI}}$  reduction observed in our  $\text{Ba}_{1-x}\text{Sr}_x\text{VS}_3$  samples is correlated to the magnetization data as follows. In Fig. 4 we report a selection of  $M(T)$  curves for three different  $x$  values in the  $x=0.06$ -0.10 region, that turns out to be critical, as shown below. For  $x \leq 0.07$ , no significant differ-

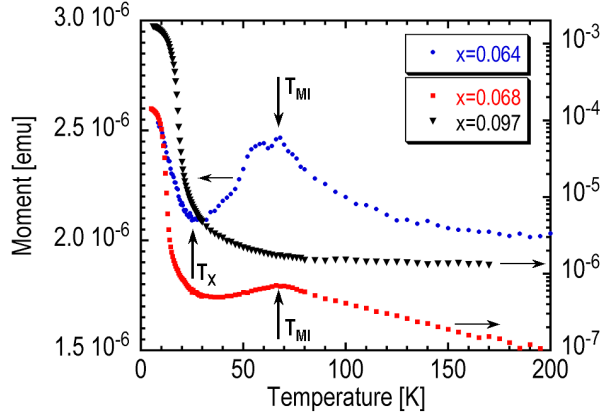


FIG. 4: ZFC magnetization for three different  $x$ -values showing the disappearance of the AF-like cusp at  $T_{\text{MI}}$  and of the upturn at  $T_{\text{X}}$  concomitant to the onset of FM order at  $x = 0.07$ . Note the different vertical scales.

ence between ZFC and FC curves is observed, so only the former case is considered. The AF-like cusp of the unsubstituted compound [3, 8] remains visible at  $T_{\text{MI}}$ , although smeared by disorder. By taking the cusp as the magnetic signature of  $T_{\text{MI}}$ , the  $T_{\text{MI}}$  vs.  $x$  magnetization data are found to coincide with the resistivity ones discussed before. The two data sets are reported in Fig. 5 and show the same monotonic decrease of  $T_{\text{MI}}$  with  $x$ . Also the upturn of the  $M(T)$  curve at  $T_{\text{X}}$  characteristic of the unsubstituted compound [7] remains visible for  $x \leq 0.07$ . Contrary to the case of the AF-like cusp, the temperature of the upturn hardly varies with  $x$  but also the upturn becomes smeared with  $x$ . At  $x_{\text{cr}} = 0.07$ , both the cusp and the upturn disappear and a FM response suddenly appears with  $T_c = 12$  K, determined as the maximum of the derivative of the  $M(T)$  curve.

The above observations lead to conclude that the MI transition is not necessarily associated with the magnetic correlations. This contrasts to the transition at  $T_{\text{X}}$  [14, 15], characterized by a FM order along the chains, in agreement with neutron diffraction data [6] and with the FM above  $x_{\text{cr}}$  presented in this letter. The analysis of several crystals with  $x \leq 0.07$  confirms the sudden character of the onset of the FM order and its coincidence with the disappearance of the AF-like cusp of and an equally sudden drop of cell volume. In the bottom panel of Fig. 3, we show the correlation between volume reduction and onset of FM order upon  $x$ . At  $x_{\text{cr}} > 0.07$ ,  $T_c$  slowly increases and equals 22 K at  $x = 0.18$ .

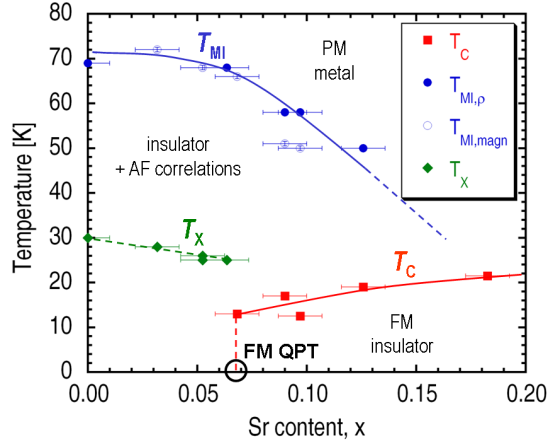


FIG. 5: Electronic phase diagram of  $\text{Ba}_{1-x}\text{Sr}_x\text{VS}_3$  at ambient pressure. Full and open circles indicate the  $T_{\text{MI}}$  values determined from, respectively, resistivity and magnetization data. The smearing of the AF-like cusp at  $T_X$  upon  $x$  discussed in the text is indicated as a broken line. The vertical line at  $x = 0.07$  marks the abrupt onset of ferromagnetic (FM) order. Lines are a guide to the eye.

Fig. 5 summarizes all data discussed above and serves as electronic phase diagram. The AF-like borderline is derived from the estimation of  $T_X$  as upturn of the magnetization. The upturn being increasingly smeared with  $x$ , as it is apparent from Fig. 4, we believe that a long range order in the ab-plane no longer exists in the substituted compounds near  $x_{\text{cr}}$ . Thus, the sudden stabilization of the FM order at  $x_{\text{cr}}$  and at low temperature is a quantum phase transition that distinguishes the FM order from a phase with AF-like correlations in the ab-plane that become weaker with increasing  $x$ . The drop of cell volume at  $x_{\text{cr}}$  appears as a structural signature of the electronic instability at room temperature.

In conclusion, we studied the effects of chemical pressure on the MI and AF-FM competitions in the  $\text{BaVS}_3$  system on a series of  $\text{Ba}_{1-x}\text{Sr}_x\text{VS}_3$  single crystals. The data of resistivity under pressure show that the Sr-induced chemical pressure stabilizes the metallic phase. Consequently, by increasing  $x$  from 0 to 0.12 the  $T_{\text{MI}}$  is reduced from 69 K down to 50 and the critical pressure for the suppression of the MI transition at 0 K decreases from 2 to 1 GPa. At  $x_{\text{cr}} = 0.07$ , we found a sudden shrinking of the unit cell concomitant to the disappearance of the AF-like susceptibility cusp at  $T_{\text{MI}}$  and to the appearance of a full FM order at low temperatures. This transition confirms the small energy difference between the AF-like and FM

orderings of the  $\text{V}^{4+}$  ions calculated ab initio [10]. By extrapolating the  $T_{\text{MI}}$  vs. V-S bond data, a metallic state at 0 K is predicted for a distance of 2.372 Å. The present data suggest that, at higher  $x$  or pressure, the FM and metallic state should coexist [15], as in  $\text{BaVS}_3$  [14, 16]. The question arises as to the mechanism leading to the FM order in our case. The absence of sulphur deficiency rules out the Hund mechanism proposed for sulphur-deficient compounds [17]. The Sr/Ba chemical disorder would favor a double-exchange mechanism, thus one should study samples without disorder. As disorder tends to stabilize the insulating state, the reduction of  $T_{\text{MI}}$  reported here is expected to be even stronger in the absence of disorder. The MI quantum phase transition predicted at  $x = 0.15$  from the data of Fig. 5 would then approach the FM QPT at  $x = 0.07$ . In the extreme case, the two points may merge, which would be important from a fundamental point of view.

The authors thank M. Marezio for useful discussions and T. Besagni for technical assistance and acknowledge financial support provided by the Consiglio Nazionale delle Ricerche.

---

Electronic address: andrea.gauzzi@upm.c.fr

- [1] R. A. Gardner, M. Vlasse and A. Wold, *Acta Cryst. B* 25, 781 (1969).
- [2] L. Forro et al., *Phys. Rev. Lett.* 85, 1938 (2000).
- [3] M. Takano et al., *J. Phys. Soc. Jpn.* 43, 1101 (1977).
- [4] T. Inami et al., *Phys. Rev. B* 66, 073108 (2002).
- [5] S. Fagot et al., *Phys. Rev. Lett.* 90, 196401 (2003).
- [6] H. Nakamura et al., *J. Phys. Soc. Japan* 69, 2763 (2000).
- [7] G. M. Italy et al., *Phys. Rev. B* 61, R7831 (2000).
- [8] O. Massenet et al., *Mat. Res. Bull.* 13, 187 (1978).
- [9] X. Jiang and G. Y. Guo, *Phys. Rev. B* 70, 35110 (2004).
- [10] A. Sanna, C. Franchini, S. Massidda, and A. Gauzzi, *Phys. Rev. B* 70, 235102 (2004).
- [11] S. Mitrovic et al., cond-mat/0502144.
- [12] F. Lechemann, S. Biermann, and A. Georges, *Phys. Rev. Lett.* 94, 166402 (2004).
- [13] A. Gauzzi et al., *Int. J. Mod. Phys. B* 17, 3503 (2003).
- [14] N. Barisic, PhD Thesis, (EPFL, Lausanne, 2004) <https://nanotubes.ep.ch/nbarisic>.
- [15] N. Barisic et al., unpublished (2005).
- [16] T. Yamasaki, S. Girit, H. Nakamura, and M. Shiga, *J. Phys. Soc. Jpn.* 70, 1768 (2001).
- [17] T. Yamasaki, H. Nakamura, and M. Shiga, *J. Phys. Soc. Jpn.* 69, 3068 (2000).